# Supporting Information

## Pd-Nanoparticles@Layered Double Hydroxide/ Reduced Graphene Oxide (Pd NPs@LDH/rGO) Nanocomposite Catalyst for Highly Efficient Green Reduction of Aromatic Nitro Compounds

Dewan Azharul Islam and Himadri Acharya*

Centre for Soft Matters, Department of Chemistry, Assam University, Silchar-788011, India. E-mail: himadriau@yahoo.co.in, himadri.acharya@aus.ac.in; Fax: +91 3842 270802; Tel: +91 3842 270848

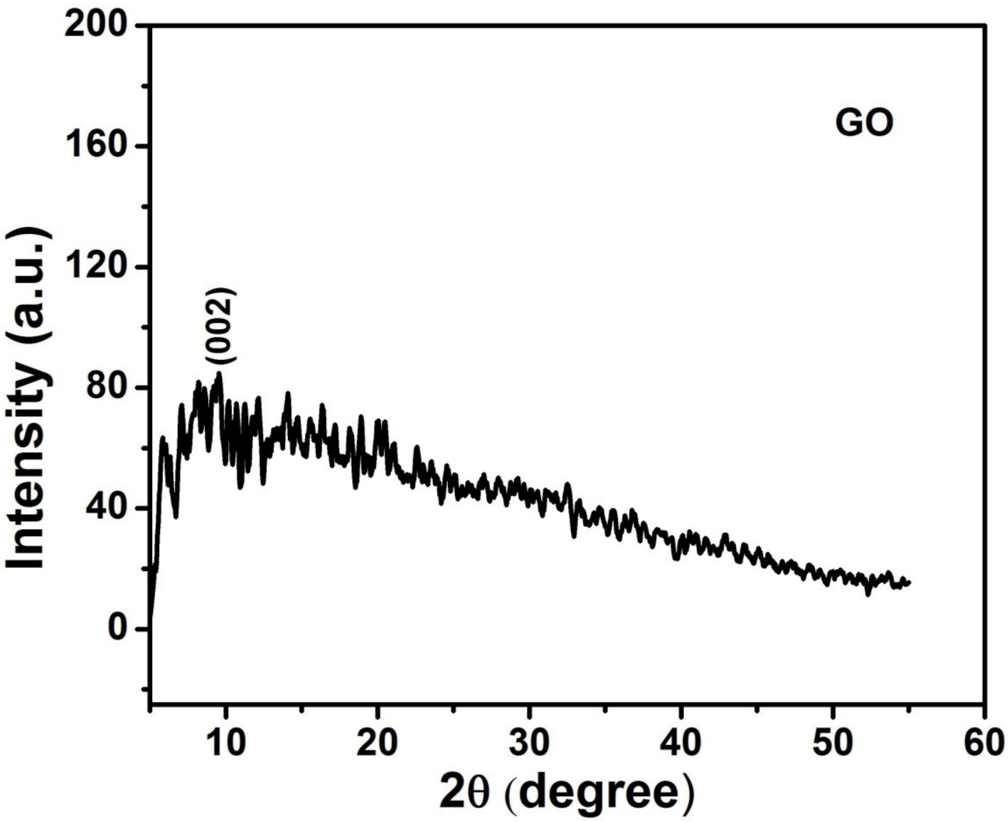


**Fig. S1** Powder XRD pattern of exfoliated GO.

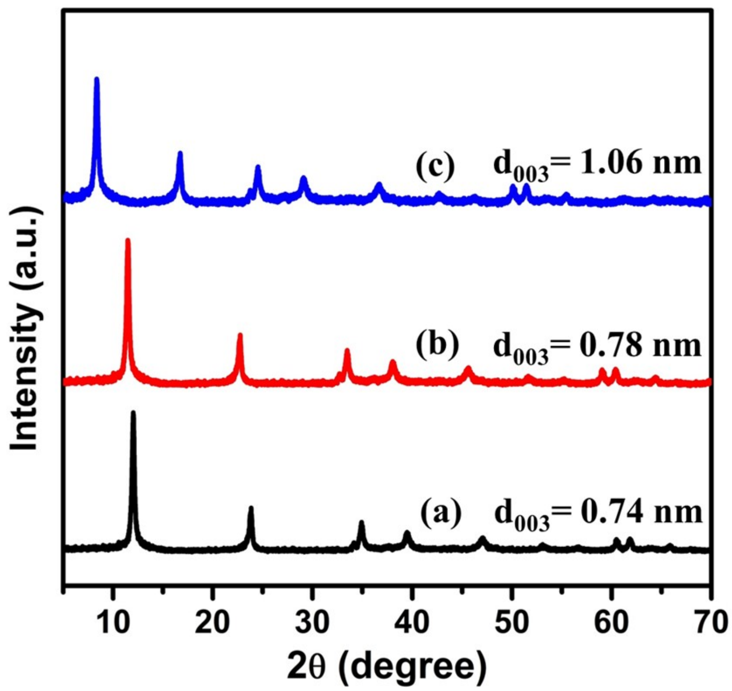


**Fig. S2** PXRD patterns of (a) ZnAl-($CO_3^{2-}$) LDH ($d_{003}$ = 0.74 nm), (b) ZnAl-($Cl^-$) LDH ($d_{003}$ = 0.78 nm) and (a) ZnAl-($PdCl_4^{2-}$) LDH ($d_{003}$ = 1.06 nm) supports successful intercalation of $PdCl_4^{2-}$ in the inter-gallery of LDH.

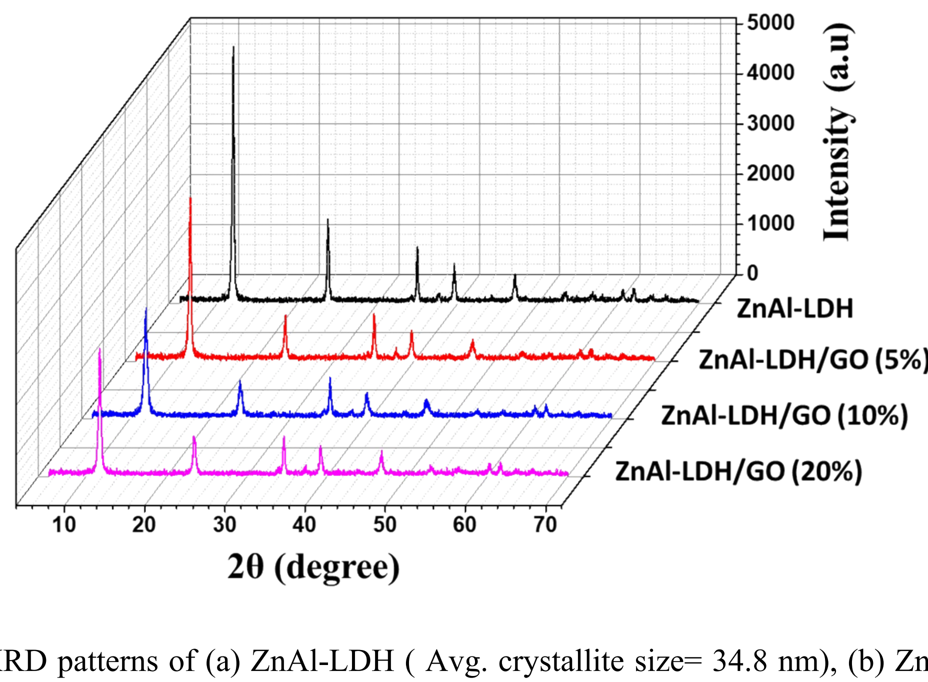


**Fig. S3** PXRD patterns of (a) ZnAl-LDH ( Avg. crystallite size= 34.8 nm), (b) ZnAl-LDH/GO (5%) (Avg. crystallite size= 27.7 nm), (c) ZnAl-LDH/GO (10%) (Avg. crystallite size= 18.2 nm) and (c) ZnAl-LDH/GO (20%) (Avg. crystallite size = 23.1 nm).

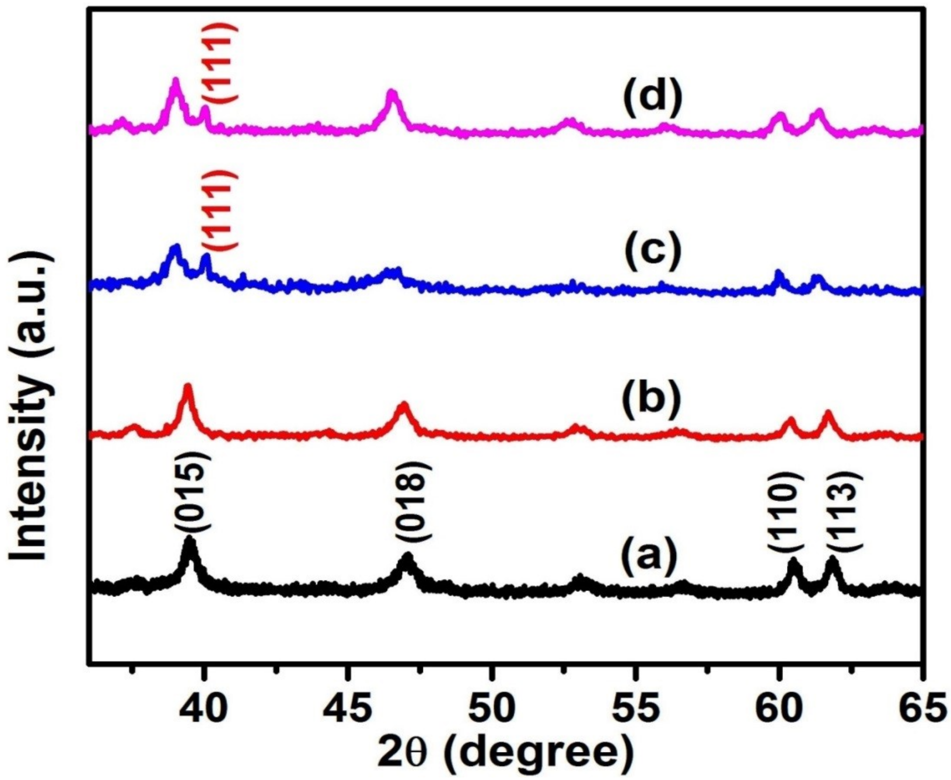


**Fig. S4** Wide angle PXRD patterns of (a) ZnAl-($CO_3^{2-}$) LDH, (b) ZnAl-($CO_3^{2-}$) LDH/GO, (c) Pd-NPs deposited ZnAl-LDH and (d) Pd-NPs deposited ZnAl-LDH/GO.

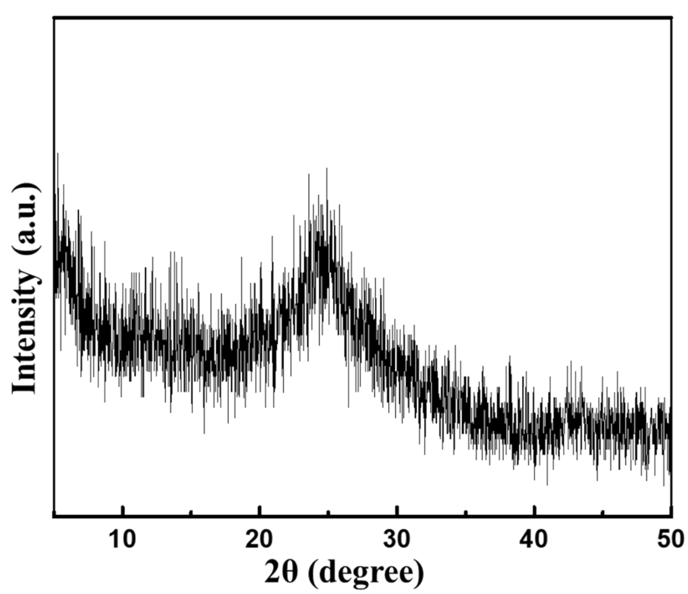


**Fig. S5** PXRD patterns of reduced graphene oxide (rGO)

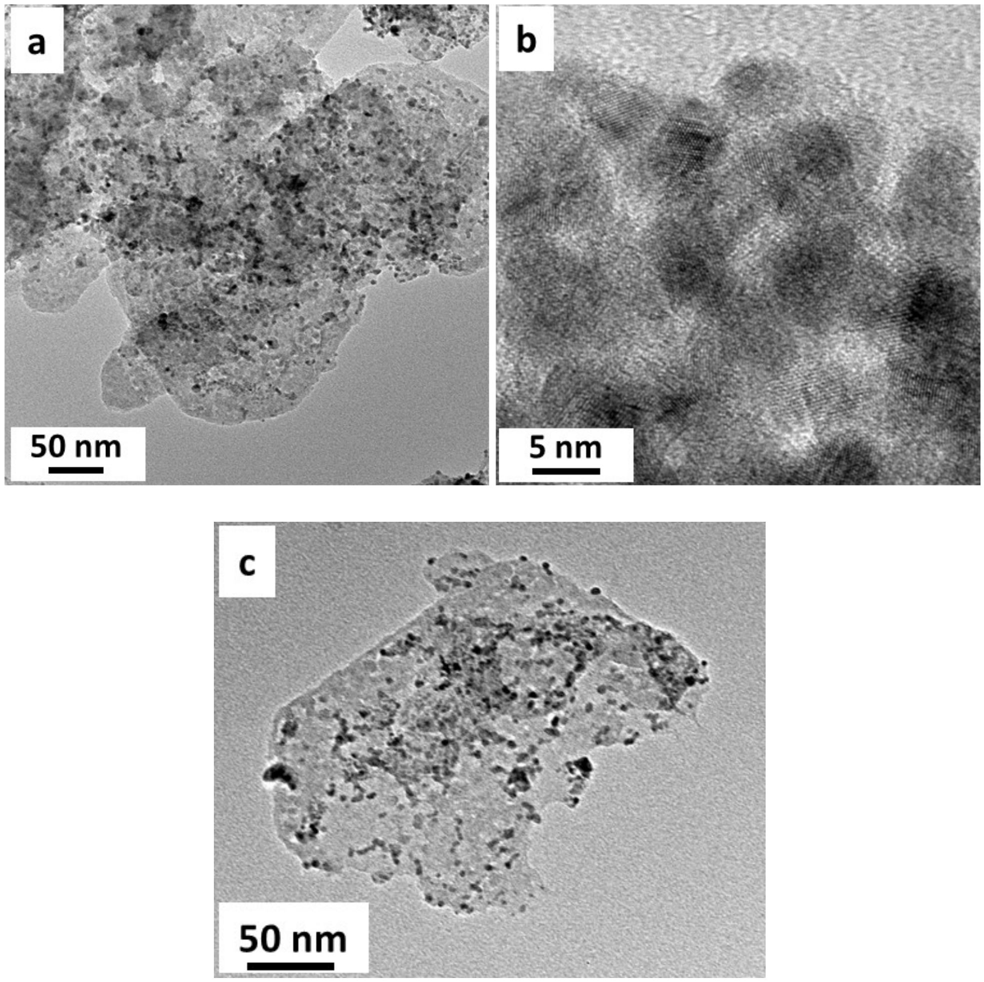


**Fig. S6** Representative TEM images of (a,b) Pd-NPs deposited on ZnAl-LDH/rGO with different magnifications (c) Pd-NPs deposited ZnAl-LDH.

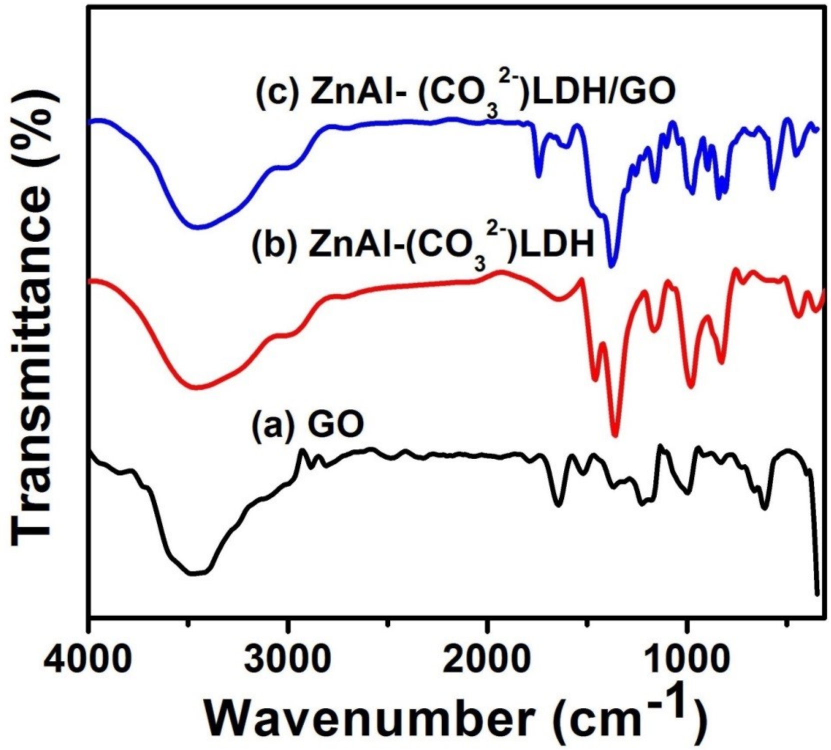


**Fig. S7** FTIR spectra of GO, ZnAl-($CO_3^{2-}$) LDH and ZnAl-($CO_3^{2-}$) LDH/GO.

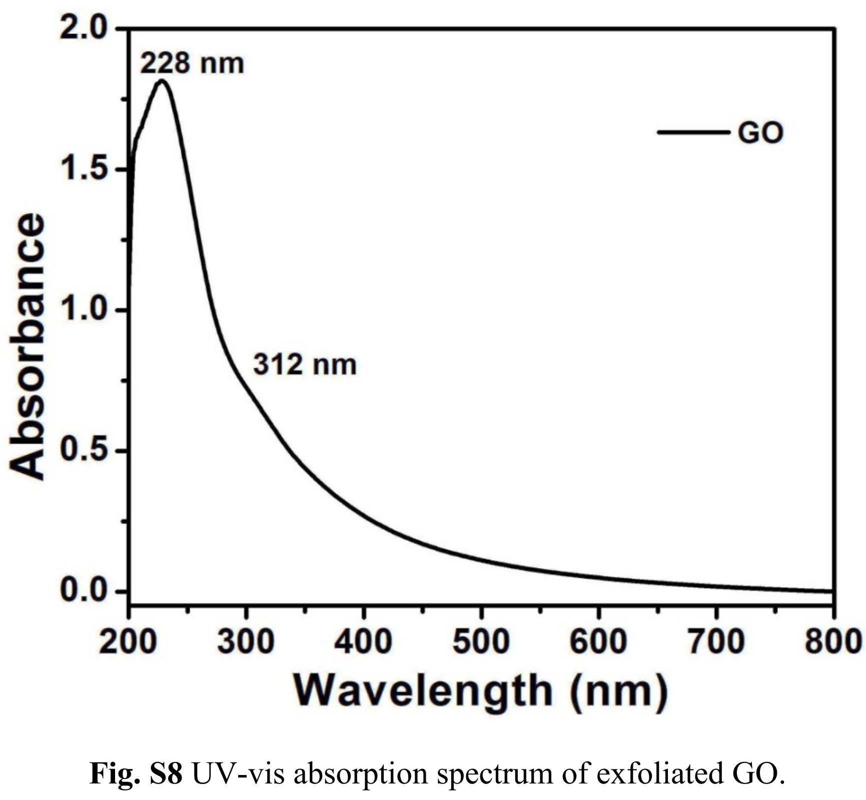


**Fig. S8** UV-vis absorption spectrum of exfoliated GO.

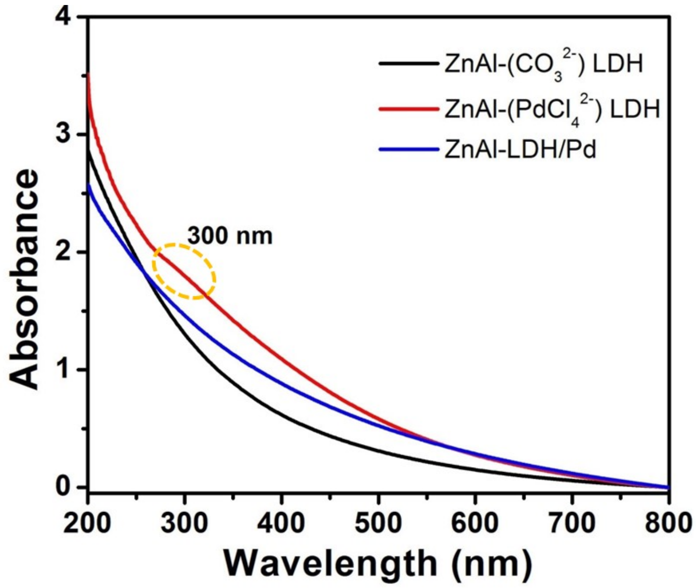


**Fig. S9** UV-vis absorption spectra of ZnAl-($CO_3^{2-}$) LDH, ZnAl-($PdCl_4^{2-}$) LDH and Pd-NPs deposited ZnAl-LDH.

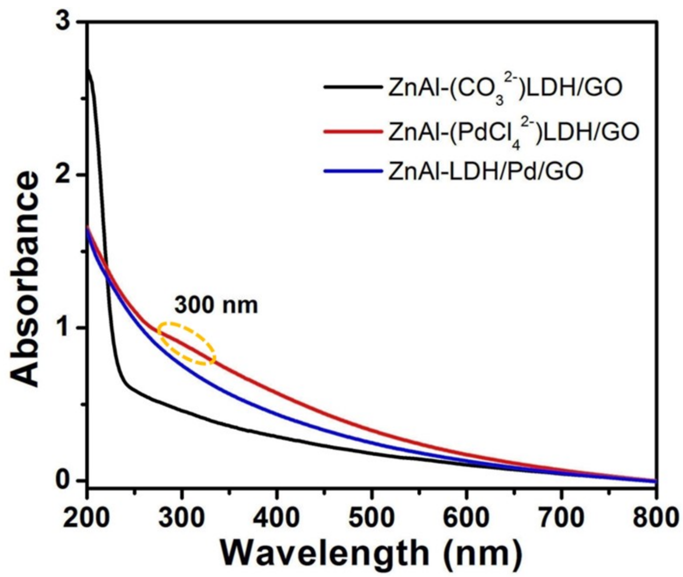


**Fig. S10** UV-vis absorption spectra of GO/ZnAl-($CO_3^{2-}$) LDH, ZnAl-($PdCl_4^{2-}$) LDH/GO and Pd-NPs deposited ZnAl-LDH/GO.

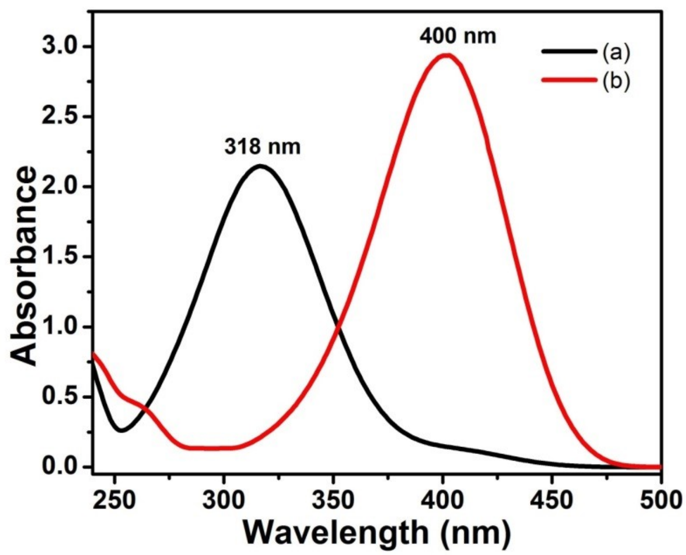


**Fig. S11** UV-vis absorption spectra of (a) 4-nitrophenol and (b) 4-nitrophenolate.

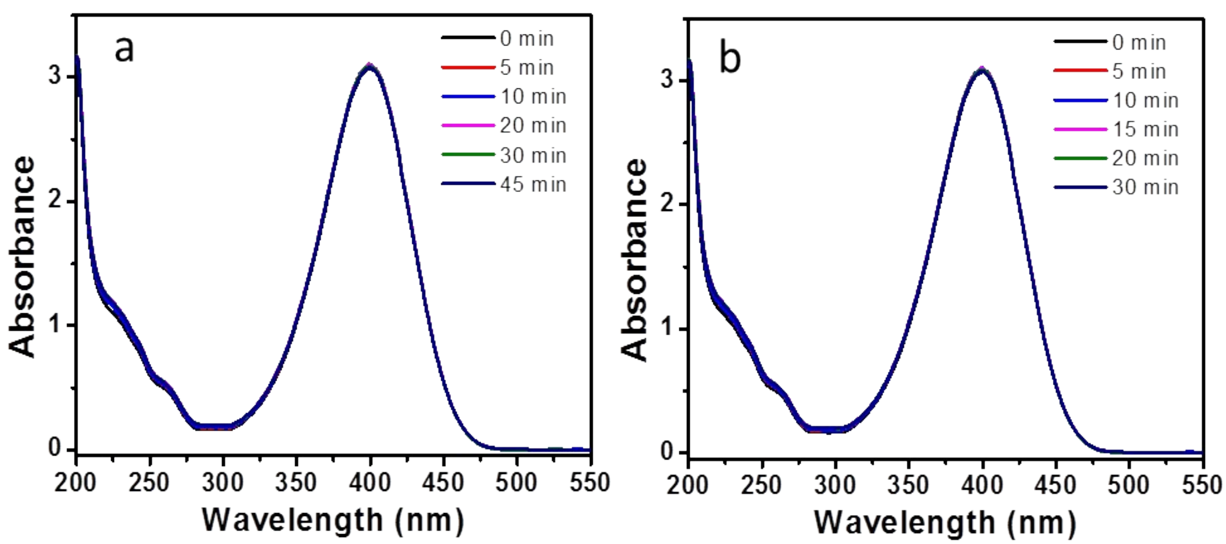


**Fig. S12** UV-vis absorption spectra during reduction of 4-nitrophenol by (a) $NaBH_4$ and (b) ZnAl-($CO_3^{2-}$) LDH catalyst.

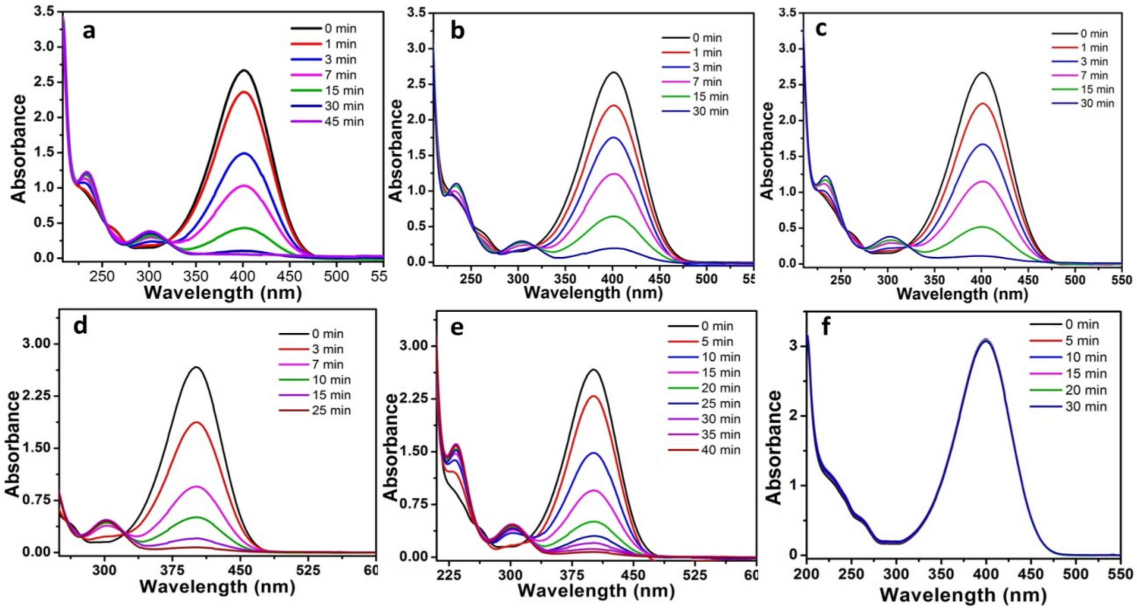


**Fig. S13** UV-vis absorption spectra during reduction of 4-nitrophenol by $NaBH_4$ in presence of (a) ZnAl-(Pd-NPs) LDH, (b) ZnAl-(Pd-NPs) LDH/GO(5%), (c) ZnAl-(Pd-NPs) LDH/GO(10%)/, (d) ZnAl-(Pd-NPs) LDH/GO(20%), (e) Pd-NPs/GO and (f) ZnAl-($CO_3^{2-}$) LDH as a catalyst.

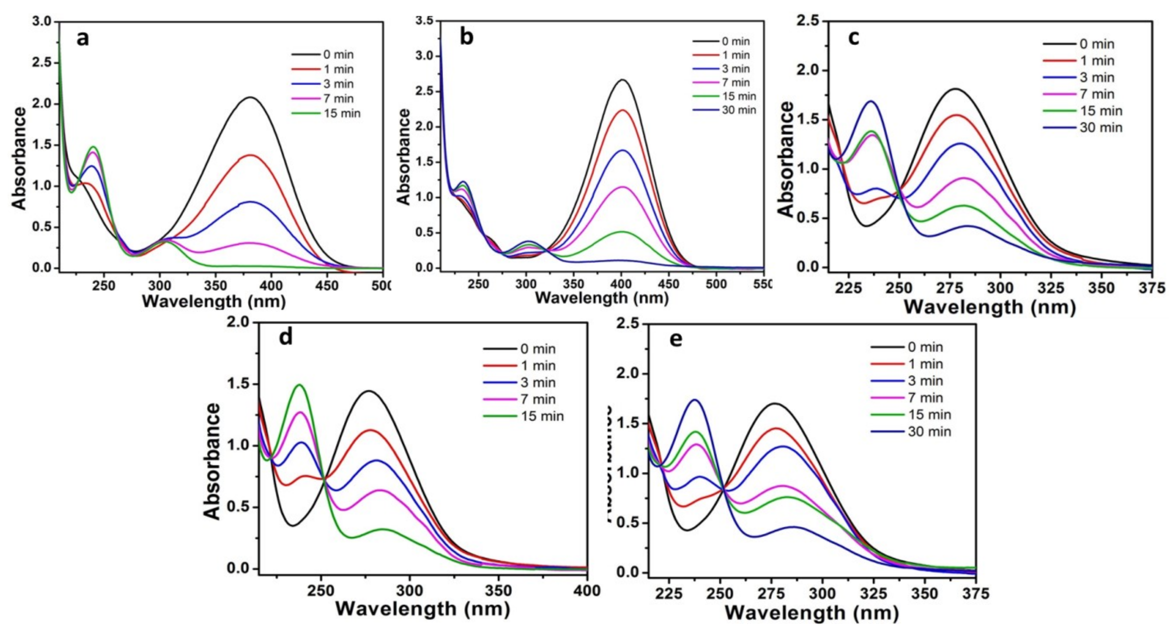


**Fig. S14** UV-vis absorption spectra during reduction of (a) 4-nitroaniline, (b) 4-nitrophenol, (c) 4-nitrobenzyl alcohol, (d) 4-nitroacetophenone and (e) 4-nitrobenzaldehyde by $NaBH_4$ in presence ZnAl-(Pd-NPs) LDH/GO as a catalyst.

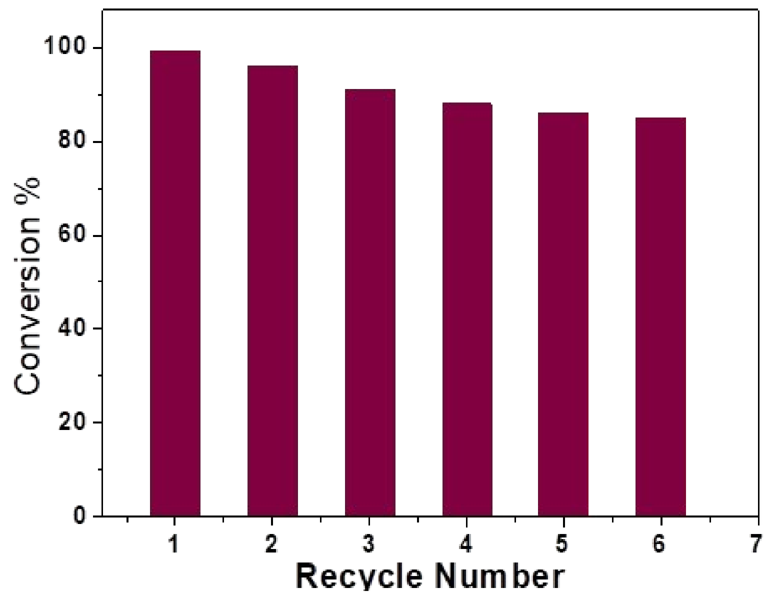


**Fig. S15** A plot of conversion (%) vs recycle number for the reduction of 4-nitroaniline over the same Pd NPs@LDH/rGO catalyst for six successive reuse cycles.

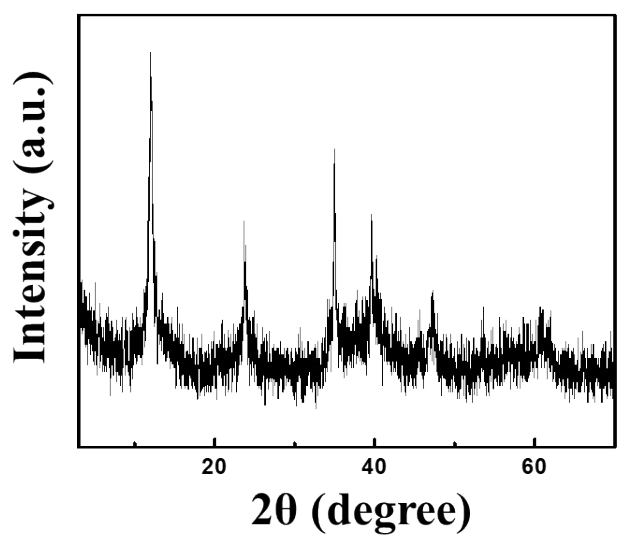


**Fig. S16** The postcatalytic PXRD pattern of reused Pd NPs@LDH/rGO catalyst after eight successive cycles.

Table-S1. Cell parameters of the synthesized compounds determined from powder X-ray diffraction.

| Compound | Cell parameter, c (nm) | Cell parameter, a (nm) |
|---|---|---|
| ZnAl($CO_3^{2-}$) LDH | 2.22 | 0.30 |
| ZnAl-($Cl^{-}$) LDHs | 2.34 | 0.30 |
| ZnAl-($PdCl_4^{2-}$) LDH | 3.18 | 0.36 |
| ZnAl($CO_3^{2-}$) LDH/GO | 2.21 | 0.30 |
| Pd@LDH | 2.20 | 0.30 |
| Pd@LDH/GO | 2.21 | 0.30 |